Nanotechnology Perceptions
ISSN 1660-6795
www.nano-*ntp.com*

Surfactant-Assisted Synthesis of Ag-Doped Zinc Oxide Nanoparticles and Their Photocatalytic Efficiency Toward Degradation of Acid Brown 14 Dye

Seema Maheshwari[a], Simrat Kaur*[a]

[a] *Department of Chemistry, Mata Gujri College, Fatehgarh Sahib-140406, Punjab, India*
**Corresponding Author's email id: chemsimrat@gmail.com*
Received: 14 August, 2018
Accepted: 7 December, 2018
https://doi.org/10.62441/nano-ntp.v14i3.5948

Zinc oxide (ZnO) and silver-doped ZnO nanoparticles stabilized with cetyltrimethylammonium bromide (CTAB) were synthesized using a sol–gel method. The structural, morphological, and optical properties of the prepared materials were examined using HRTEM, FTIR, UV–visible, and fluorescence spectroscopy. HRTEM results revealed nearly spherical nanoparticles forming trigonal nanostructures with an average size of around 18 nm and clear lattice fringes indicating a crystalline hexagonal wurtzite structure. FTIR analysis confirmed the presence of functional groups and successful CTAB capping on the nanoparticle surface. Optical studies demonstrated that Ag incorporation influences the electronic properties of ZnO. The photocatalytic activity of the nanoparticles was evaluated through the degradation of Acid Brown 14 dye under irradiation. CTAB-ZnO achieved 86.9% degradation, while CTAB-Ag-ZnO showed enhanced efficiency of 93.2%, mainly due to improved charge separation and reduced electron–hole recombination. These findings indicate that CTAB-stabilized Ag-doped ZnO nanoparticles are promising photocatalysts for dye removal from wastewater.

KEYWORDS Nanoparticles, doping, surfactant, Zinc Oxide, CTAB, Silver, Photocatalytic efficiency.

1. INTRODUCTION

Water contamination by synthetic dyes has become one of the most significant environmental challenges associated with industrial development. Large volumes of coloured effluents are generated from textile, leather, paper, printing, and dye manufacturing industries, where dyes are widely used for coloring fabrics and other materials. It is estimated that nearly 10–15% of the total dye production is lost during textile processing and released into wastewater streams, leading to severe environmental pollution [1], [2]. These dyes are intentionally formulated to remain stable and resist degradation by light, heat, and microorganisms. As a result, they can persist in aquatic environments, reducing light penetration and disrupting photosynthetic processes in water bodies [3], [4]. Among various classes of dyes, azo dyes constitute the largest group, accounting for approximately 60–70 % of the total dye production worldwide.

These dyes contain one or more azo groups (–N=N–) linking aromatic rings, which provide strong color and chemical stability but also contribute to their recalcitrance in wastewater treatment processes [5]. Conventional wastewater treatment methods such as coagulation–flocculation, adsorption, filtration, and biological treatment are often inadequate for removing azo dyes due to their complex and stable structures. Therefore, advanced oxidation processes (AOPs) have gained attention as an effective alternative, as they produce highly reactive hydroxyl radicals (•OH) capable of oxidizing organic pollutants into harmless products like carbon dioxide, water, and inorganic ions [6]. Among the various AOPs, heterogeneous semiconductor photocatalysis has emerged as an efficient and environmentally friendly technology for wastewater remediation [7] [8]. Several semiconductor materials including TiO_2, ZnO, CdS, WO_3, and Fe_2O_3 have been investigated for photocatalytic degradation of organic pollutants [9], [10], [11]. Among them, zinc oxide (ZnO) has attracted considerable attention due to its advantageous physicochemical properties such as a wide band gap (~3.37 eV), high exciton binding energy (~60 meV), chemical stability, non-toxicity, and relatively low cost [12], [13]. ZnO nanostructures also exhibit strong oxidation capability and high electron mobility, making them effective photocatalysts for the degradation of various organic contaminants in water [14]. Additionally, ZnO nanoparticles can be synthesized using a wide range of techniques including sol–gel, hydrothermal, precipitation, and solvothermal methods, enabling control over particle size, morphology, and surface characteristics [15]. Numerous studies have demonstrated that ZnO nanomaterials exhibit significant photocatalytic activity toward the degradation of dyes such as methylene blue, methyl orange, and other azo dyes [16], [17], [18]. Although ZnO offers several advantages as a photocatalyst, its practical performance is often restricted by inherent limitations. A major challenge is the fast recombination of photogenerated electron–hole pairs, which decreases the number of active charge carriers available for redox reactions and consequently reduces the overall photocatalytic efficiency [19], [20]. In addition, the relatively wide band gap of ZnO restricts its photoresponse primarily to the ultraviolet region, which constitutes only a small fraction of the solar spectrum [21]. To overcome these limitations, various modification strategies have been explored to enhance the photocatalytic performance of ZnO nanomaterials. These strategies include metal doping, non-metal doping, surface modification, and heterojunction formation with other semiconductors. Among these approaches, doping with noble metals such as silver (Ag), gold (Au), or platinum (Pt) has proven particularly effective [22]. Metal doping can introduce defect states within the semiconductor structure and facilitate charge separation by acting as electron traps, thereby suppressing electron–hole recombination. Silver, in particular, has been widely used because of its excellent electrical conductivity and ability to enhance interfacial charge transfer processes [23]. Experimental studies have shown that Ag-doped ZnO exhibits superior photocatalytic activity compared with pure ZnO, primarily due to reduced electron–hole recombination and improved surface catalytic properties. In addition to metal doping, the use of surfactants during synthesis has been recognized as an effective approach for controlling the size, morphology, and dispersion of nanoparticles. Among various surfactants, cetyltrimethylammonium bromide (CTAB) is widely used due to its strong ability to stabilize nanoparticles and prevent agglomeration. CTAB molecules adsorb onto the surface of growing particles, reducing surface energy and enabling controlled growth of nanostructures with improved dispersion and uniformity. It also facilitates interaction between

the catalyst surface and organic dye molecules. The combination of surfactant capping and metal doping therefore provides a synergistic strategy for improving the photocatalytic performance of ZnO-based nanomaterials. Combining Ag doping with CTAB-assisted synthesis is expected to improve photocatalytic performance through multiple mechanisms, including enhanced charge separation, increased surface area, improved adsorption of dye molecules, and better dispersion of nanoparticles.

In this context, the present study focuses on the synthesis and characterization of CTAB-capped Ag-doped ZnO nanoparticles and their application in the photocatalytic degradation of Acid Brown 14 dye in aqueous solution. The structural, morphological, and optical properties of the synthesized nanomaterials are characterized using techniques such as Fourier transform infrared spectroscopy (FTIR), EM), and UV–visible spectroscopy. The photocatalytic activity of the prepared catalysts is evaluated through degradation experiments under light irradiation, and the degradation kinetics are analyzed to assess catalytic efficiency. The results are expected to provide insights into the synergistic effects of Ag doping and CTAB capping in enhancing the photocatalytic performance of ZnO nanomaterials for environmental remediation applications.

2. Reagents and Solutions

All chemicals employed in this study were of analytical grade and were used without any further purification, as supplied by Sigma-Aldrich. Triply distilled water was utilized for preparing all solutions. Zinc acetate [$Zn(CH_3COO)_2 \cdot 2H_2O$] (>98%), Silver nitrate anhydrous [$AgNO_3$] (>98%), Ammonium Hydroxide (NH_4OH) and Cetyltrimethylammonium Bromide [$C_{16}H_{33}–N^+(CH_3)_3\ Br^-$] (CTAB, MW: 364.45 g) (≥ 99%), Ethanol (absolute, >99.8%), The glassware used in this experimental work were acid washed. Triply Distilled water was used for all dilution and sample preparation.

3. Apparatus

The synthesized materials were characterized using several analytical techniques, including UV–visible spectroscopy, fluorescence spectroscopy, Fourier transform infrared (FT-IR) spectroscopy, and High-Resolution Transmission Electron Microscopy (HRTEM). The FT-IR spectra were obtained using a Bruker FT-IR spectrometer over the wavenumber range of 400–4000 cm^{-1}, employing the KBr pellet method for sample preparation. The size of the synthesized material was determined by HRTEM using model TALOS F200S G2200 KV, FEG, CMOS Camera 4Kx4K. For HRTEM analysis, the diluted nanoparticles were suspended in ethanol and introduced on a copper grid, and the analysis was carried out after drying them in air. The optical absorption spectra of the samples dispersed in triply distilled water were recorded using a Shimadzu UV-1700 UV–Visible spectrophotometer. Fluorescence measurements were carried out with a Shimadzu RF-5301PC spectrofluorophotometer (Shimadzu, Japan) equipped with a 150 W xenon arc lamp as the excitation source. Quartz cuvettes with a 1 cm path length were used for recording the spectra. The slit widths for the excitation and emission monochromators were typically adjusted to 5 nm during the

measurements. Prior to analysis, the nanoparticle suspensions were dispersed using an ultrasonic bath (Sarthak Scientific Services, India) to ensure uniform distribution of particles in the solution. All optical measurements were conducted under ambient laboratory conditions.

4. Methods for synthesis of CTAB capped Ag doped ZnO nanomaterials:

Synthesis of CTAB capped Ag doped ZnO nanoparticles (CTAB-Ag-ZnO): Ag doped ZnO nanoparticles capped with CTAB were synthesized by a sol-gel route. Ethanol and Zinc acetate were dissolved by taking 6.96 g of Zinc acetate in 50ml of ethanol under continuous stirring to obtain a uniform solution. An appropriate amount of anhydrous silver nitrate corresponding to 2 mol % with respect to Zinc, was added to this mixture. In a dropping funnel, 2g of capping agent (CTAB) mixed with 2ml hydrochloric acid in 50 ml distilled water were placed. The resulting solution was then introduced dropwise into the Zinc acetate solution. To Ph of the solution was brought to 9 by adding NH_4OH solution. The reaction mixture was heated at 100°C on a water bath for 30 min, resulting in the formation of CTAB-Ag-ZnO. The synthesized sol-gel was then centrifuged to 4000rpm, the precipitates thus obtained was dried. Similarly, the sample of CTAB-ZnO was prepared by the same process without using siver nitrate for doping. A schematic representation of the synthesis process is shown in Figure 1.

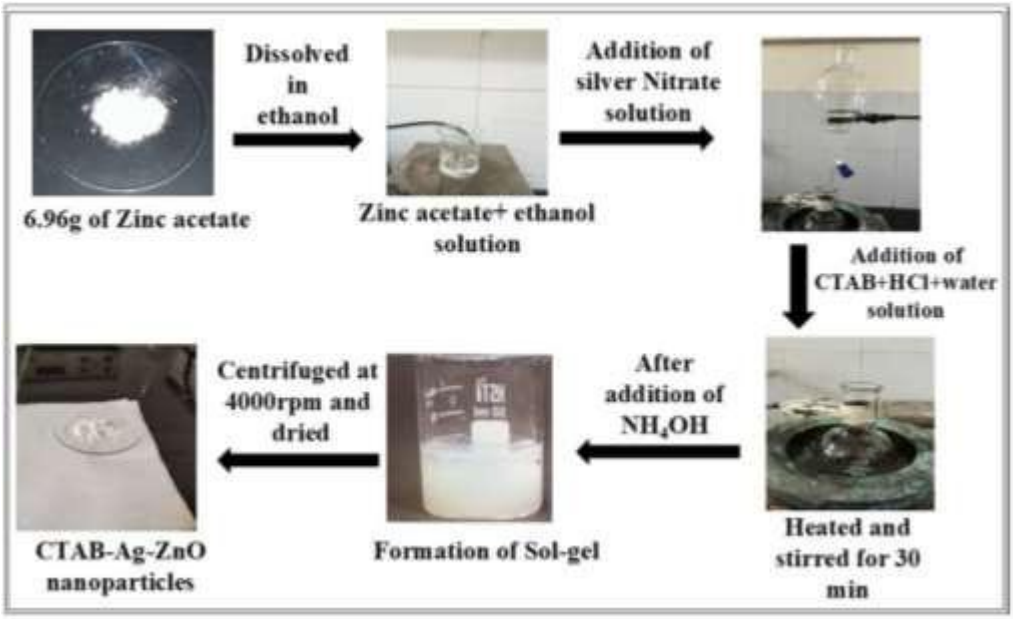

Figure 1: Schematic diagram showing steps for the synthesis of CTAB-Ag-ZnO.

5. Result and discussion

Characterizing nanostructures is crucial for examining their optical and morphological features and determining their potential for various applications. A thorough analysis of nanoparticles typically involves multiple analytical and spectroscopic approaches. In this study, the synthesized nanoparticles were characterized using the following techniques.

5.1 IR Spectra

The FTIR spectrum of CTAB-Ag-ZnO and CTAB-ZnO nanoparticles offers valuable insight into the surface functional groups and verifies the attachment of the capping agent on the nanoparticles surface (shown in figure 2). The observed absorption bands mainly arise from hydroxyl groups, vibrations of the long hydrocarbon chain of CTAB, and the characteristic lattice vibration of Zn–O bonds. A broad band appearing in the region 3300–3400 cm^{-1} is commonly associated with the O–H stretching vibration of surface hydroxyl groups and physically adsorbed water molecules present on the ZnO nanoparticles. This feature indicates the presence of moisture and hydroxylated surfaces [24]. Peaks observed near 2935 cm^{-1} and 2840 cm^{-1} correspond to the asymmetric and symmetric stretching vibrations of $–CH_2$ groups, respectively, which originate from the long alkyl chain of the CTAB molecule [25]. These bands confirm that the surfactant molecules are associated with the nanoparticle surface.

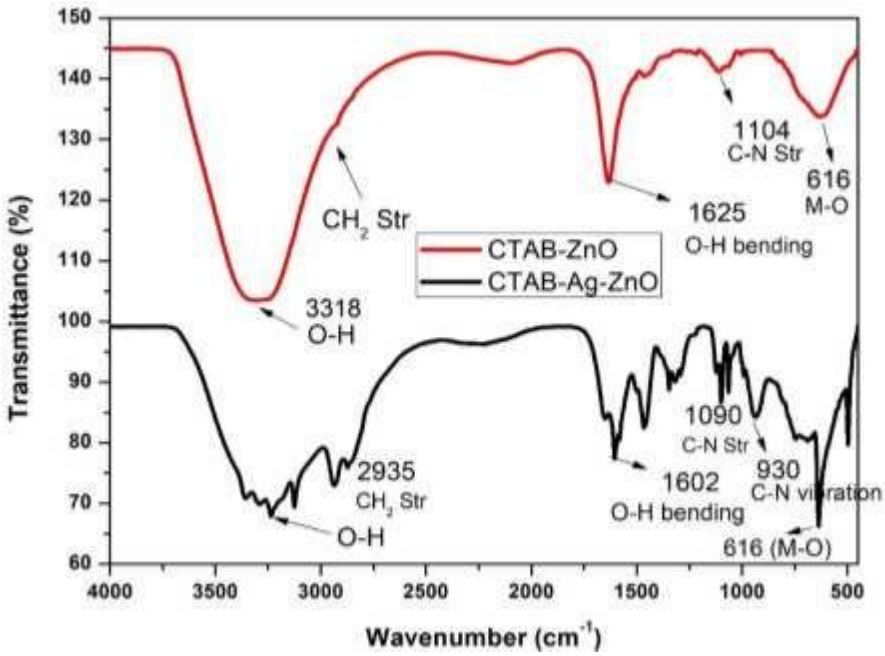

Figure 2: IR Spectra of CTAB-ZnO and CTAB-Ag-ZnO.

A band around 1600–1625 cm^{-1} is generally attributed to the bending vibration of H–O–H, indicating the presence of adsorbed water. The band appearing between 1110–1080 cm^{-1} is related to the C–N stretching vibration of the quaternary ammonium group in CTAB, suggesting interaction between the positively charged head group and the ZnO surface [26]. The most distinctive feature of ZnO nanoparticles appearing at 616 cm^{-1}, corresponds to the Zn–O stretching vibration of the crystal lattice [27]. This band serves as clear evidence for the formation of ZnO nanostructures and demonstrates that CTAB molecules are successfully adsorbed on the surface of ZnO nanoparticles. The surfactant therefore acts as an effective

stabilizing and capping agent, limiting particle aggregation and influencing the surface chemical environment of the nanomaterial.

5.2 UV Spectra

The UV–visible absorption spectra of CTAB-ZnO and CTAB-Ag-ZnO was recorded to study the optical properties shown in Figure 3. The spectra display a distinct absorption maximum at 294 nm for CTAB-ZnO, which is attributed to the fundamental band-to-band electronic transition of ZnO nanocrystals. In contrast, CTAB-Ag-ZnO nanoparticles exhibit a slightly blue-shifted absorption peak at 291 nm. This shift toward lower wavelength indicates changes in the electronic environment of ZnO caused by the incorporation of Ag ions, which may introduce lattice distortions or alter the particle size and defect structure [28]. The CTAB molecules serve as a surface capping and stabilizing agent, helping to prevent particle aggregation while also modifying the surface states of the nanoparticles, thereby influencing their optical absorption properties.

The optical band gap of these nanomaterials can be determined using the Tauc relation, where $(\alpha h\nu)^2$ is plotted against the photon energy ($h\nu$), considering ZnO as a direct band gap semiconductor. The band gap energy is obtained by extrapolating the linear portion of the Tauc plot to the point where $(\alpha h\nu)^2$ becomes zero on the energy axis. Based on this analysis, the estimated band gap values are approximately 4.22 eV for CTAB-ZnO (with absorption at 294 nm) and 4.26 eV for CTAB-Ag- ZnO (with absorption at 291 nm). The marginal increase in band gap observed for the doped sample is consistent with the blue shift in the absorption spectrum and may result from doping-induced alterations in the band structure along with quantum confinement effects present in the nanocrystalline material [29].

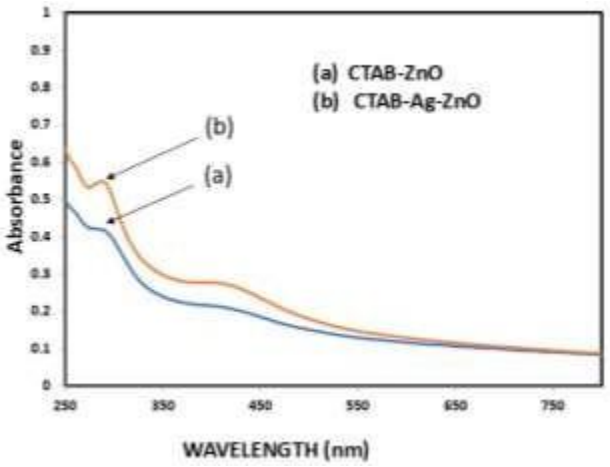

Figure 3: UV-Visible spectra of CTAB-ZnO and CTAB-Ag-ZnO.

5.3 Fluorescence Spectra

The fluorescence spectrum of CTAB-ZnO nanoparticles typically displays an emission band associated with near band-edge transitions along with defect-induced luminescence. When Silver is introduced into the ZnO lattice, distinct variations in the photoluminescence behaviour become evident. Compared to CTAB-ZnO nanoparticles, the CTAB-Ag-ZnO sample exhibits a noticeable shift of the emission peak from 340 nm to 361nm as shown in Figure 4. The shift toward longer wavelength (red shift) accompanied by a decline in fluorescence intensity. This shift can be linked to the formation of impurity states and slight lattice distortions resulting from Ag incorporation, which modify the band structure and influence charge carrier recombination pathways [30]. At the same time, the reduction in emission intensity indicates that Ag ions may function as trapping sites for electrons, promoting non-radiative recombination and thereby diminishing radiative electron–hole transitions [31]. Furthermore, the CTAB molecules present on the nanoparticle surface contribute to particle stabilization and alter surface defect states, which also impacts the emission properties [32]. Collectively, the observed red shift and quenching of fluorescence suggest effective incorporation of Ag within the ZnO lattice and highlight its influence on the optical characteristics of the nanoparticles.

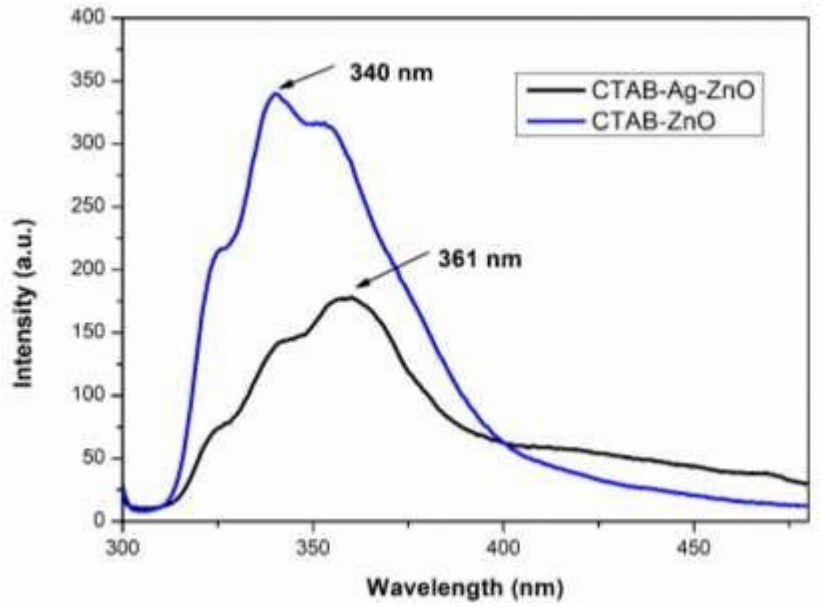

Figure 4: Fluorescence spectra of UV-Visible spectra of CTAB-ZnO and CTAB-Ag-ZnO at λ_{ex} of 260nm and slit width of 5nm.

5.4 HRTEM

High-resolution transmission electron microscopy (HRTEM) was employed to investigate the morphology and microstructural characteristics of CTAB-Ag-ZnO nanoparticles shown in Figure 5. The HRTEM images reveal that the material consists predominantly of nearly

spherical nanoparticles, which tend to assemble and aggregate to form trigonal nanostructured arrangements. The average particle size of the nanoparticles is found to be approximately 18 nm, indicating the formation of nanoscale crystallites with relatively uniform dimensions. Clear and well-defined lattice fringes are visible in the HRTEM micrographs, confirming the crystalline nature of the synthesized nanoparticles. The measured interplanar spacing (d-spacing) of about 0.59 nm corresponds to specific crystallographic planes of ZnO, supporting the formation of a well-ordered crystal lattice. This spacing is characteristic of the hexagonal wurtzite crystal structure, which is the most stable phase of ZnO [33]. The observed lattice fringes and ordered atomic arrangement further verify the high crystallinity of the nanoparticles. Overall, the HRTEM analysis demonstrates that CTAB-assisted synthesis leads to the formation of Ag-doped ZnO nanoparticles with spherical morphology that self-assemble into trigonal nanostructures while maintaining the characteristic wurtzite phase of ZnO.

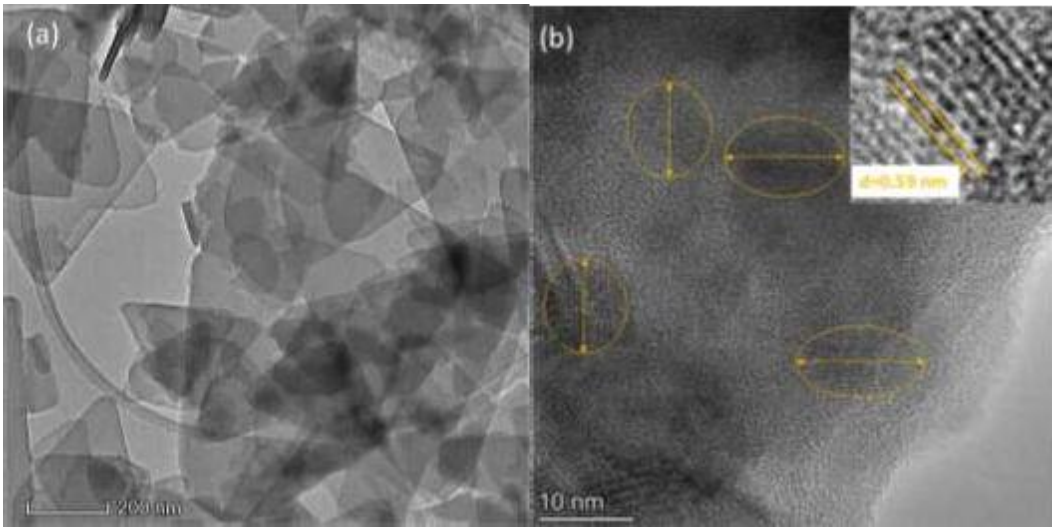

Figure5: HRTEM images of CTAB-Ag-ZnO (a) showing trigonal nanostructures at 200nm scale (b) showing spherical nanoparticles at the scale of 10nm.

6. Photodegradation studies:

For the photocatalytic degradation study, an aqueous solution of Acid Brown 14 dye was prepared using 10 mg of nanocatalyst (CTAB–ZnO and CTAB–Ag–ZnO) was suspended in a 100 mL solution of the dye (10 mg/L) solution in water. Before light exposure, the mixture was kept under dark conditions for 20 mins to achieve adsorption–desorption equilibrium between the dye molecules and the catalyst surface. After this equilibration step, the initial absorbance of the dye solution was recorded using UV–visible spectroscopy. Subsequently, the suspension was exposed to a simulated UV-Visible light (300–800 nm) light source to initiate photocatalytic degradation. At regular intervals, small portions of the reaction mixture were withdrawn, centrifuged to remove the catalyst particles, and analyzed spectrophotometrically as shown in Figure 6. The progress of degradation was monitored by

observing the gradual decrease in the characteristic absorption peak of the dye, and the degradation efficiency was determined by comparing the absorbance values before and after irradiation.

The degradation process occurs through a photocatalytic mechanism in which light irradiation excites electrons from the valence band of ZnO to the conduction band, generating electron–hole pairs [34]. These charge carriers participate in surface reactions that produce reactive oxygen species such as superoxide and hydroxyl radicals. These highly reactive species attack the dye molecules, breaking down their complex structure into smaller and less harmful products. The incorporation of silver enhances the photocatalytic performance by promoting efficient separation of photogenerated charge carriers and suppressing their recombination, thereby increasing the formation of reactive radicals [17]. Consequently, CTAB-Ag–ZnO nanoparticles exhibit improved efficiency for the degradation of Acid Brown 14 dye compared with CTAB-ZnO.

Photodegradation Efficiency (%) = $[(A_o - A_t) / A_o] \times 100$

Where, Ao is the initial absorbance (before degradation), A[t=30 min] is the absorbance after degradation at time t.

In case of CTAB-ZnO from figure 6 (a) the initial concentration of AB14 dye, Ao is 0.8104 and A[t=30mins] is 0.055 at λmax = 488 nm. The % Degradation obtained is 86.9%. whereas for CTAB-Ag-ZnO figure 6 (b) the initial absorbance, Ao is 0.8104 and Final absorbance, A after 30 min is 0.106 at λmax 488 nm. The % Degradation was found to be 93.2%.

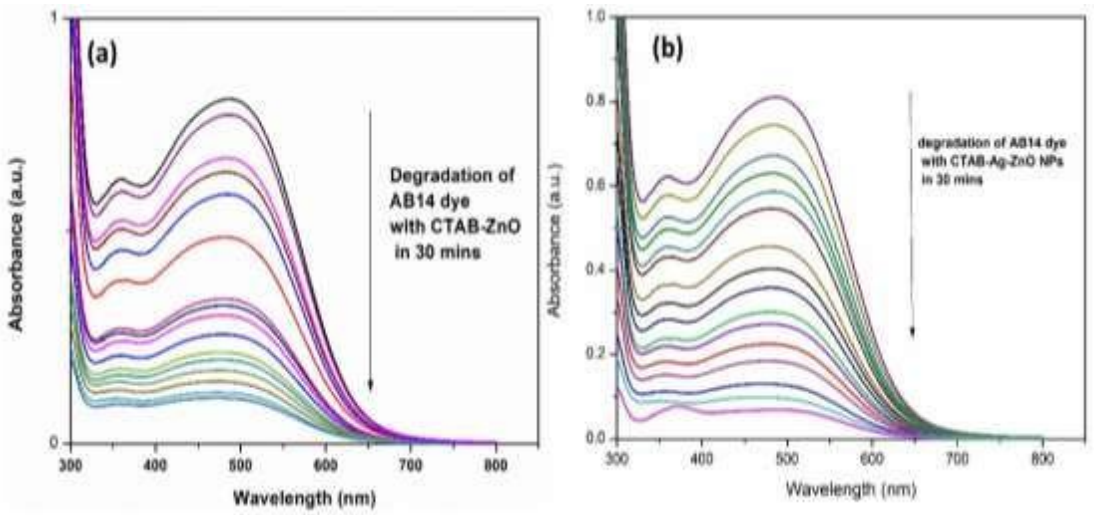

Figure 6: Degradation studies of AB14 dye (a) Degradation by CTAB-ZnO (b) Degradation by CTAB-Ag-ZnO in 30 mins.

7 Conclusion:

CTAB-capped ZnO and silver-doped ZnO nanoparticles were synthesized using a sol–gel technique and subsequently characterized to examine their structural and optical features. Analytical techniques including HRTEM, FT-IR, UV–visible spectroscopy, and fluorescence spectroscopy confirmed the formation of nanostructured materials and the successful surface stabilization by CTAB. The optical investigations further indicated that the incorporation of silver enhances the optical response of ZnO nanoparticles. The photocatalytic activity was investigated through the degradation of Acid Brown 14 dye under light irradiation. The CTAB-Ag-ZnO demonstrated higher degradation efficiency (93.2%) compared with the CTAB–ZnO nanoparticles (86.9%). Overall, the results highlight that Ag incorporation along with CTAB capping improves both the optical behaviour and photocatalytic efficiency of ZnO nanoparticles, making CTAB–Ag–ZnO a promising material for wastewater dye remediation.

Acknowledgements
All the authors thank the Chemistry Department, Mata Gujri College, Fatehgarh Sahib for providing the laboratory and instrument facilities.

Declarations:
Ethical Approval There is no ethical approval required.

Consent To Participate: All authors give consent to participate in the revision of the manuscript.

Consent To Publish: All authors give consent to publish the paper. Competing Interests The authors declare no competing interests.

References:

[1] T. Robinson, G. McMullan, R. Marchant, P. Nigam, Remediation of dyes in textile effluent: a critical review on current treatment technologies with a proposed alternative, Bioresour. Technol., 77 (2001) 247–255.
[2] E. Forgacs, T. Cserháti, G. Oros, Removal of synthetic dyes from wastewaters: a review, Environ. Int., 30 (2004) 953–971.
[3] U. Shanker, M. Rani, V. Jassal, Degradation of hazardous organic dyes in water by nanomaterials, Environ. Chem. Lett., 15 (2017) 623–642.
[4] B.S. Padhi, Pollution due to synthetic dyes toxicity & carcinogenicity studies and remediation, Int. J. Environ. Sci., 3 (2012) 940.
[5] N. Dafale, S. Wate, S. Meshram, N.R. Neti, Bioremediation of wastewater containing azo dyes through sequential anaerobic–aerobic bioreactor system and its biodiversity, Environ. Rev., 18 (2010) 21–36.
[6] J.L. Wang, L.J. Xu, Advanced Oxidation Processes for Wastewater Treatment: Formation of Hydroxyl Radical and Application, Crit. Rev. Environ. Sci. Technol., 42 (2012) 251–325.

[7] S.N. Ahmed, W. Haider, Heterogeneous photocatalysis and its potential applications in water and wastewater treatment: a review, Nanotechnology, 29 (2018) 342001.
[8] Y. Nosaka, A.Y. Nosaka, Generation and Detection of Reactive Oxygen Species in Photocatalysis, Chem. Rev., 117 (2017) 11302–11336.
[9] C.C. Nguyen, Novel strategies to develop efficient titanium dioxide and graphitic carbon nitride-based photocatalysts, (2018).
[10] X. Liu, Tunability of photogenerated charge carrier density on semiconductors by in-situ electrochemical treatments, PhD Thesis, University of British Columbia, 2018.
[11] A. Deb, Photocatalytic degradation of Benzophenone 3 in aqueous media under UV light irradiation, (2018).
[12] S.G. Kumar, K.K. Rao, Zinc oxide based photocatalysis: tailoring surface-bulk structure and related interfacial charge carrier dynamics for better environmental applications, Rsc Adv., 5 (2015) 3306–3351.
[13] A comprehensive review of ZnO materials and devices | Journal of Applied Physics | AIP Publishing, (n.d.).
[14] M.A. Mohd Adnan, N.M. Julkapli, S.B. Abd Hamid, Review on ZnO hybrid photocatalyst: impact on photocatalytic activities of water pollutant degradation, Rev. Inorg. Chem., 36 (2016).
[15] X. Wang, M. Ahmad, H. Sun, Three-dimensional ZnO hierarchical nanostructures: solution phase synthesis and applications, Materials, 10 (2017) 1304.
[16] L.V. Trandafilović, D.J. Jovanović, X. Zhang, S. Ptasińska, M.D. Dramićanin, Enhanced photocatalytic degradation of methylene blue and methyl orange by ZnO: Eu nanoparticles, Appl. Catal. B Environ., 203 (2017) 740–752.
[17] X. Chen, Z. Wu, D. Liu, Z. Gao, Preparation of ZnO Photocatalyst for the Efficient and Rapid Photocatalytic Degradation of Azo Dyes, Nanoscale Res. Lett., 12 (2017) 143.
[18] Solar Photocatalytic Degradation of Azo Dye: Comparison of Photocatalytic Efficiency of ZnO and TiO2 | Request PDF, (n.d.).
[19] M.A. Johar, R.A. Afzal, A.A. Alazba, U. Manzoor, Photocatalysis and Bandgap Engineering Using ZnO Nanocomposites, Adv. Mater. Sci. Eng., 2015 (2015) 1–22.
[20] M.A. Mohd Adnan, N.M. Julkapli, S.B. Abd Hamid, Review on ZnO hybrid photocatalyst: impact on photocatalytic activities of water pollutant degradation, Rev. Inorg. Chem., 36 (2016).
[21] S.K. Mishra, R.K. Srivastava, h S. Prakash, ZnO nanoparticles: Structural, optical and photoconductivity characteristics, J. Alloys Compd., 539 (2012) 1–6.
[22] H. Liu, J. Feng, W. Jie, A review of noble metal (Pd, Ag, Pt, Au)–zinc oxide nanocomposites: synthesis, structures and applications, J. Mater. Sci. Mater. Electron., 28 (2017) 16585–16597.
[23] C. Karunakaran, V. Rajeswari, P. Gomathisankar, Optical, electrical, photocatalytic, and bactericidal properties of microwave synthesized nanocrystalline Ag–ZnO and ZnO, Solid State Sci., 13 (2011) 923–928.
[24] S.B. Rana, Influence of CTAB assisted capping on the structural and optical properties of ZnO nanoparticles, J. Mater. Sci. Mater. Electron., 28 (2017) 13787–13796.

[25] M. Khan, C. Wei, M. Chen, J. Tao, N. Huang, Z. Qi, L. Li, CTAB-mediated synthesis and characterization of ZnO/Ag core–shell nanocomposites, J. Alloys Compd., 612 (2014) 306–314.
[26] S. Muniyappan, T. Solaiyammal, B.G.T. Keerthana, P. Vivek, P. Murugakoothan, Influence of annealing temperature on structural, morphological and optical properties of CTAB assisted cadmium sulphide (CdS) quantum dots: promising candidate for quantum dot sensitized solar cell (QDSSC) applications, J. Mater. Sci. Mater. Electron., 28 (2017) 11317–11324.
[27] S.S.T. Selvi, J.M. Linet, S. Sagadevan, Influence of CTAB surfactant on structural and optical properties of CuS and CdS nanoparticles by hydrothermal route, J. Exp. Nanosci., 13 (2018) 130–143.
[28] Synthesis, structural and optical properties of Ag doped ZnO nanoparticles with enhanced photocatalytic properties by photo degradation of organic dyes | Journal of Materials Science: Materials in Electronics | Springer Nature Link, (n.d.).
[29] S.M. Hosseini, I.A. Sarsari, P. Kameli, H. Salamati, Effect of Ag doping on structural, optical, and photocatalytic properties of ZnO nanoparticles, J. Alloys Compd., 640 (2015) 408–415.
[30] V. Kumar, J. Prakash, J.P. Singh, K.H. Chae, C. Swart, O.M. Ntwaeaborwa, H.C. Swart, V. Dutta, Role of silver doping on the defects related photoluminescence and antibacterial behaviour of zinc oxide nanoparticles, Colloids Surf. B Biointerfaces, 159 (2017) 191–199.
[31] T.N. Ravishankar, K. Manjunatha, T. Ramakrishnappa, G. Nagaraju, D. Kumar, S. Sarakar, B.S. Anandakumar, G.T. Chandrappa, V. Reddy, J. Dupont, Comparison of the photocatalytic degradation of trypan blue by undoped and silver-doped zinc oxide nanoparticles, Mater. Sci. Semicond. Process., 26 (2014) 7–17.
[32] D. Verma, A.K. Kole, P. Kumbhakar, Red shift of the band-edge photoluminescence emission and effects of annealing and capping agent on structural and optical properties of ZnO nanoparticles, J. Alloys Compd., 625 (2015) 122–130.
[33] M. Anbuvannan, M. Ramesh, G. Viruthagiri, N. Shanmugam, N. Kannadasan, Synthesis, characterization and photocatalytic activity of ZnO nanoparticles prepared by biological method, Spectrochim. Acta. A. Mol. Biomol. Spectrosc., 143 (2015) 304–308.
[34] Q. Li, Z.-L. Fan, D.-X. Xue, Y.-F. Zhang, Z.-H. Zhang, Q. Wang, H.-M. Sun, Z. Gao, J. Bai, A multi-dye@MOF composite boosts highly efficient photodegradation of an ultra-stubborn dye reactive blue 21 under visible-light irradiation, J. Mater. Chem. A, 6 (2018) 2148–2156.